Hydrogen Effect on Phase Transition Temperature of HANA-6

Tian Chen [a], Dongju Kim [a], Youho Lee [a*]
[a]*Seoul National University, Seoul, Republic of Korea.*
[*]*Corresponding author: leeyouho@snu.ac.kr*

***Keywords: Phase transformation, HANA-6, DSC, hydrogen**

1. Introduction

Zirconium-based (Zr) alloys are the predominant materials for nuclear fuel cladding due to their low thermal absorption cross-section, excellent mechanical properties and reliable corrosion resistance under normal operating conditions. However, during the service life of fuel cladding in light water reactors (LWRs), the cladding undergoes environmental degradation, most notably through the absorption of hydrogen generated by the cladding-coolant water reaction. This hydrogen uptake leads to the formation of brittle hydrides once the terminal solid solubility (TSS) is exceeded, which can significantly compromise the mechanical integrity of the fuel rods, particularly under accident scenarios [1], [2].

Among various safety-critical events, the Loss-of-Coolant Accident (LOCA) is of primary concern. During a LOCA transient, the cladding temperature rises rapidly, triggering a solid-state phase transformation from the hexagonal close-packed (HCP) α-phase to the body-centred cubic (BCC) β-Zr phase. This transformation is a pivotal event in safety analysis; the β-phase exhibits oxygen diffusion coefficient orders of magnitude higher than those of the α-phase, leading to accelerated steam oxidation and potential embrittlement. Furthermore, the α→β transition is accompanied by significant changes in creep behaviour and thermal expansion, which directly affect cladding ballooning and rupture behaviour.

Hydrogen is widely recognised as a potent β-stabiliser that lowers both the onset ($T_{\alpha/\alpha+\beta}$) and offset ($T_{\alpha+\beta/\beta}$) temperatures of the phase transformation. While this effect is well-documented for conventional alloys like Zircaloy-4, modern reactor designs increasingly utilise advanced Nb-modified alloys for higher burnup efficiency. HANA-6 (Zr-1.1Nb-0.05Cu), developed in South Korea, is one such alloy. Unlike conventional alloys typically utilised in the fully recrystallised (RXA) or cold-worked stress-relieved (CWSR) states, the HANA-6 utilised in this study is in the partially recrystallised (PRXA) state, which may influence its phase stability.

This study aims to address the gap in knowledge regarding the impact of hydrogen and oxygen on the phase transition temperature of HANA-6 using differential scanning calorimetry (DSC). The findings are compared with literature data for conventional Zr alloys to enhance the understanding of phase transformation behaviours in advanced alloys under operational and accident conditions, particularly LOCA scenarios.

2. Experimental

2.1 Materials

The chemical composition of the Zr alloy used in this study is summarised in Table 1. Specimens were obtained from reactor-grade HANA-6 (PRXA) and ZIRLO (CWSR) cladding tubes. To evaluate the individual and combined effects of interstitials, three sets of HANA-6 specimens were prepared:

1) Hydrogen-charged HANA-6: 91.2 to 1902.1 wppm.
2) Oxygen-charged HANA-6: 0.56 to 2.13wt.%;
3) Combined H/O HANA-6: hydrogen (43.2 – 1068.8 wppm) and oxygen (0.17 – 3.18wt.%).

Additionally, ZIRLO specimens were charged with hydrogen (70.7 to 1185.7 wppm) to serve as a comparative baseline.

Table I: Chemical composition of Zr alloys in this study.

Element (%)	Sn	Nb	Cu	Fe	Cr	Zr
HANA-6	-	1.1	0.05	-	-	Bal.
ZIRLO	0.5	0.98	-	0.11	-	Bal.

2.2 Interstitial Charging and Homogenisation

Oxygen charging was conducted via high-temperature steam oxidation at 1200˚C, followed by an annealing process at 1200˚C in an inert atmosphere to ensure a homogenous distribution. Hydrogen was introduced using a high-temperature gas-charging system at 400˚C. Final concentrations were verified using a hot vacuum extraction analyser (ELTRA ONH-2000).

2.3 Differential Scanning Calorimetry (DSC)

Calorimetric measurements were performed using a NETZSCH DSC 404 F3 Pegasus at a heating rate of 20˚C/min under a high-purity argon environment. The

onset and offset temperatures were determined using the tangential intersection method.

3. Results and Discussion

3.1 Comparison of Hydrogen Sensitivity

The DSC results in **Figure 1** reveal a significant disparity in hydrogen sensitivity between the two alloys. For ZIRLO (CWSR), the $T_{\alpha/\alpha+\beta}$ decreases sharply with increasing hydrogen content, reflecting the standard β-stabilising effect: the $T_{\alpha/\alpha+\beta}$ decreased by approximately 185˚C at ~1000 wppm H.

However, this study identifies a unique hydrogen-insensitivity in the HANA-6 alloy. Contrary to conventional thermodynamic expectations for Zr-Nb alloys, the $T_{\alpha/\alpha+\beta}$ of HANA-6 decreased by only 22˚C even as hydrogen content reached 1902.1 wppm. This finding suggests that the β-stabilising efficiency of hydrogen is fundamentally suppressed in the HANA-6, compared to ZIRLO and other conventional literature benchmarks.

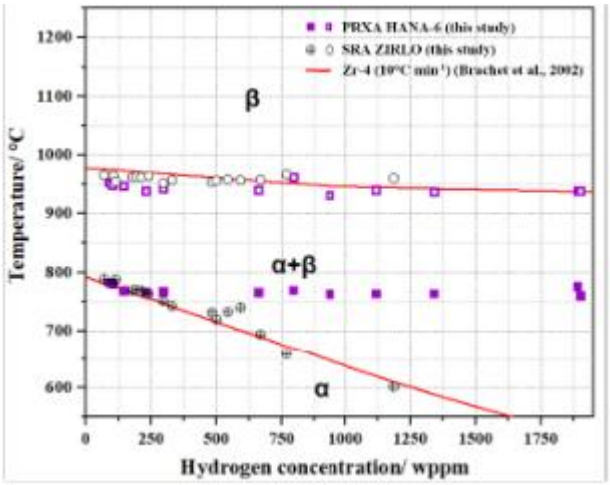

Fig. 1. Psuedobinary zircaloy-hydrogen phase diagram of Zircaloy-4 (Brachet et al., 2002) [3], ZIRLO (this study) and HANA-6 (this study).

3.2 Influence of Oxygen on Phase Transformation

The influence of oxygen content on the α→β transformation boundaries of HANA-6 is shown in **Figure 2**. Consistent with literature data for Zircaloy-4 [4], [5] and other Nb-modified alloys [6] (e.g., M5), oxygen acts as a potent β-stabiliser, shifting the transformation temperatures upward as concentration increases.

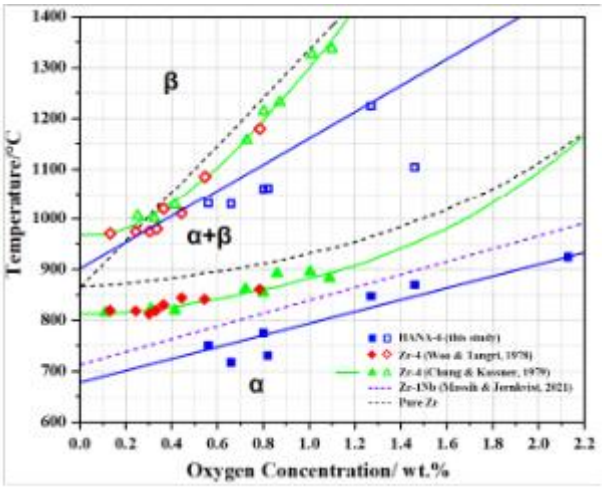

Fig. 2. Pseudobinary zircaloy-oxygen phase diagram. Lines represent empirical correlations, while symbols denote experimental data.

3.3 Combined Influence of Hydrogen and Oxygen

The combined effects of hydrogen and oxygen on HANA-6 are presented in **Figure 3**. The data are categorised into three hydrogen concentration windows: 0 – 100 wppm (black), 100 – 400 wppm (red) and 400 – 700 wppm (blue).

Two primary trends emerge from this analysis. First, oxygen acts as a strong α-stabiliser, where both $T_{\alpha/\alpha+\beta}$ and $T_{\alpha+\beta/\beta}$ rise with increasing oxygen, especially beyond approximately 1 wt.% O. Second, at a fixed oxygen level, increasing hydrogen content clearly shifts both phase boundaries to lower temperatures. This behaviour is consistent with the established role of hydrogen as a β-stabiliser.

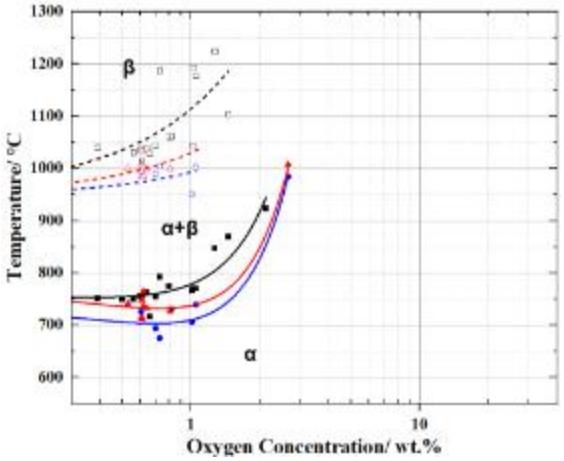

Fig. 3. Effect of oxygen concentration on the $T_{\alpha+\beta}$ of HANA-6 at different hydrogen levels. For each hydrogen range, the $T_{\alpha/\alpha+\beta}$ was fitted with solid lines, while the $T_{\alpha+\beta/\beta}$ by dashed lines.

Notably, this behaviour represents a critical contrast to the results obtained from the hydrogen-only specimens discussed in Section 3.1, where the transformation temperatures barely shifted. To

investigate this apparent contradiction, the thermal history of the oxygen-charged proves involved a post-oxidation annealing step at 1200˚C for homogenisation. It was hypothesised that this thermal treatment altered the as-received PRXA microstructure in a way that restored the β-stabilising effect of hydrogen.

To test this hypothesis, the hydrogenated specimens were subjected to a controlled recrystallisation heat treatment at 600˚C for 4 hours to produce a fully recrystallisation (RXA) microstructure. As shown in **Figure 4**, the behaviour of the RXA specimens (pink diamond) changed dramatically compared to the as-received PRXA state (purple square). In the RXA state, the onset boundary decreased systematically with hydrogen content, following the trends established for Zircaloy-4 and ZIRLO. This comparison confirms that the anomalous hydrogen insensitivity in as-received HANA-6 is not an intrinsic alloy property, b specifically linked to its partially recrysta microstructure. The reappearance of the hydrogen in oxygen-charged specimens is thus explained b full recrystallisation that occurred during the 12 homogenisation process.

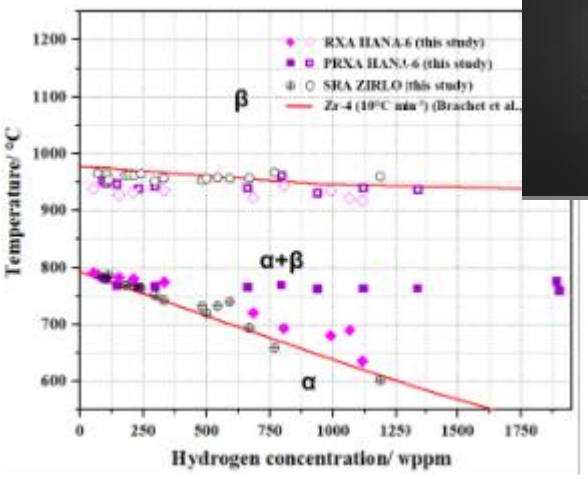

Fig. 4. Updated Pseudobinary Zircaloy-Hydrogen Phase Diagram with recrystallised HANA-6 (this study).

3.4 Microstructural Analysis and Strain-Mediated Sequestration Mechanism

To investigate the origin of the reduced hydrogen sensitivity observed in PRXA HANA-6 during DSC measurements, Transmission Electron Microscopy (TEM) analysis was conducted on hydrogen-charged specimen.

Bright-field imaging (**Figure 5a, b**) shows a high density of dislocation tangles and sub-grain boundaries, characteristic of the partially recrystallised microstructure. These defects introduce local lattice distortion and generate heterogenous elastic strain fields within the α-Zr matrix. FFT analysis of defect-rich regions (**Figure 5c**) reveals spot broadening and diffuse reciprocal-space intensity, indicating local variations in lattice periodically consistent with strain gradients associated with dislocation structures.

Hydrogen in α-Zr has a positive partial molar volume and therefore interacts elastically with the surrounding stress field. Regions experiencing reduced elastic constraint provide energetically favourable sites for hydrogen accommodation. As a result, the defect rich PRXA microstructure is expected to promote hydrogen partitioning into these regions. Such strain-assisted trapping can reduce the effective hydrogen supersaturation in the matrix and thereby influence subsequent hydride precipitation behaviour. This strain-mediated sequestration provides a plausible microstructural basis for altered hydrogen response in the PRXA condition.

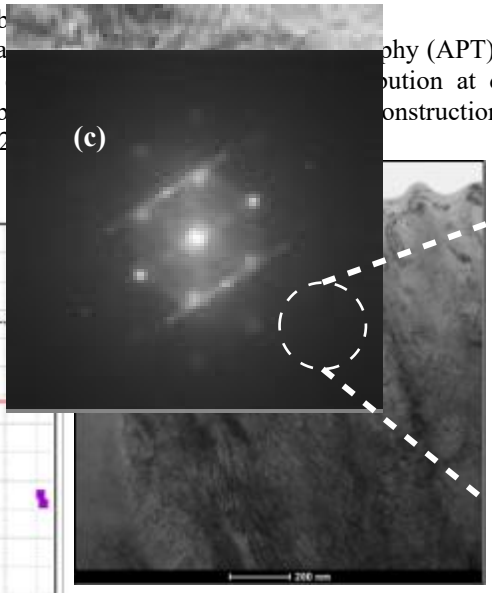

Fig. 5. (a) Bright-field TEM image of PRXA HANA-6 showing a high density of dislocation tangles and sub-grain boundaries. The circled region indicates the area selected for FFT analysis. (b) Higher magnification image highlighting defect clusters characteristic of the partially recrystallised microstructure. (c) FFT of the defect-rich region showing spot broadening and diffuse reciprocal-space intensity, consistent with local lattice distortion and heterogenous elastic strain field.

4. Conclusion

This study demonstrates that PRXA HANA-6 exhibits reduced sensitivity of the α→β phase transformation temperature to hydrogen content up to 1902.1 wppm H. In contrast, ZIRLO follows the conventional behaviour, exhibiting a sharp decrease in transformation temperatures as hydrogen content increases. Oxygen increases the transition temperatures as expected; however, after thermal homogenisation process at 1200˚C, the β-stabilising effect of hydrogen to reappears. Recrystallisation experiments (600˚C for

4h) confirm that the hydrogen anomaly is governed by the PRXA microstructural state. Once the alloy is fully recrystallised, it recovers its conventional sensitivity to hydrogen.

ACKNOWLEDGEMENT

This work was supported by the Korea Institute of Energy Technology Evaluation and Planning(KETEP) and the Ministry of Climate, Energy & Environment(MCEE) of the Republic of Korea (No. RS-2022-KP002856).

REFERENCES

[1] T. P. Chapman, D. Dye, and D. Rugg, “Hydrogen in Ti and Zr alloys: Industrial perspective, failure modes and mechanistic understanding,” *Philosophical Transactions of the Royal Society A: Mathematical, Physical and Engineering Sciences*, vol. 375, no. 2098. 2017. doi: 10.1098/rsta.2016.0418.

[2] A. T. Motta *et al.*, “Hydrogen in zirconium alloys: A review,” *Journal of Nuclear Materials*, vol. 518. 2019. doi: 10.1016/j.jnucmat.2019.02.042.

[3] J. C. Brachet *et al.*, “Influence of Hydrogen Content on the α/β Phase Transformation Temperatures and on the Thermal-Mechanical Behavior of Zy-4, M4 (ZrSnFeV), and M5 (ZrNbO) Alloys During the First Phase of LOCA Transient,” 2002. [Online]. Available: https://api.semanticscholar.org/CorpusID:137184526

[4] O. T. Woo and K. Tangri, “Transformation characteristics of rapidly heated and quenched zircaloy-4-oxygen alloys,” *J. Nucl. Mater.*, vol. 79, no. 1, 1979, doi: 10.1016/0022-3115(79)90435-5.

[5] H. M. Chung and T. F. Kassner, “Pseudobinary Zircaloy-Oxygen Phase Diagram,” *J. Nucl. Mater.*, vol. 84, no. 1–2, 1979, doi: 10.1016/0022-3115(79)90172-7.

[6] A. R. Massih and L. O. Jernkvist, “Solid state phase transformation kinetics in Zr-base alloys,” *Sci. Rep.*, vol. 11, no. 1, 2021, doi: 10.1038/s41598-021-86308-w.